The Astrophysical Journal, 634:L121–L124, 2005 November 20

MAGNETIC RECONNECTION FLUX AND CORONAL MASS EJECTION VELOCITY

Jiong Qiu[1,2,3] and Vasyl B. Yurchyshyn[1]

Received 2005 August 19; accepted 2005 October 11; published 2005 November 10

ABSTRACT

We explore the relationship between the total reconnection flux $\psi_{\rm rec}$ estimated from flare observations and the velocity $V_{\rm CME}$ of coronal mass ejections (CMEs) observed with the Large Angle and Spectrometric Coronagraph (LASCO) Experiment. Our study includes 13 events with varying magnetic configurations in source regions. It is shown that $V_{\rm CME}$ is proportional to $\psi_{\rm rec}$, with a linear cross-correlation of 89% and confidence level greater than 99.5%. This result confirms the importance of magnetic flux transferred by magnetic reconnection in the early stage of fast CMEs. On the other hand, the CME velocity and kinematic energy are probably independent of magnetic configurations of source regions.

Subject headings: Sun: activity — Sun: coronal mass ejections (CMEs) — Sun: flares — Sun: magnetic fields

1. INTRODUCTION

Magnetic reconnection is considered to play an important role in the early stage of many large-scale solar eruptions. In our previous studies on solar eruptive events consisting of coronal mass ejections (CMEs), flares, and filaments, we found evident temporal correlations and magnitude scaling relationships between filament acceleration and the rate of magnetic reconnection inferred from flare observations (Qiu et al. 2004; Jing et al. 2005). However, a direct comparison between CME acceleration and reconnection rate is not conclusive, as in the studied events, CME observations with the Large Angle and Spectrometric Coronagraph (LASCO) Experiment start at 2–3 solar radii, when the stage of fast acceleration is nearly terminated (Zhang et al. 2001). In this Letter, we derive the total reconnection flux as the time integration of the reconnection rate and compare it with the mean velocity of CMEs spanning from 2 to 30 solar radii as observed by LASCO C2 and C3. CMEs at this stage are just coming out of the fast acceleration phase and usually exhibit no acceleration or very small deceleration. Therefore, the mean CME velocity during this stage is close to the maximum CME speed. This approach removes the very large uncertainties in determining the start times of CMEs and allows us to make a direct comparison between the reconnection and kinematics of CMEs.

It should be noted that the amount of total reconnection flux is an important physical parameter interacting with flux rope evolution. Independent of specific low-corona magnetic configurations of source regions, magnetic reconnection reconstructs the magnetic topology in a way that most probably helps diminish the tension force binding the flux rope plasma to the solar surface, thus enhancing the upward motion of the flux rope. The amount of mass and magnetic flux exchanged between the flux rope and its ambience is nonnegligible.

The reconnection rate can be inferred as

$$\varphi_{\rm rec} = \frac{\partial}{\partial t}\left(\int B_n\, dA\right),$$

where dA is the newly brightened flare area at each instant and B_n is the normal component of magnetic fields encompassed by dA (Forbes & Lin 2000 and references therein). This relationship is valid given that the following assumptions hold. Magnetic flux is conserved from the photosphere to the corona. The photospheric magnetic fields are line-tied, or equivalently, their evolution timescale is much longer than the reconnection timescale. Heating of the lower atmosphere during flares is an immediate response to magnetic reconnection at the corona, which transports energy downward. And the timescales of magnetic reconnection, energy transport, and heating of lower atmosphere are shorter than the observation and/or measurement timescales. Realistically, the timescale of magnetic field evolution ranges from hours to days, and timescales of magnetic reconnection, energy transfer, and atmosphere heating range from a fraction of a second to a few seconds. Meanwhile, our observation or measurement timescale is from several seconds to 3 minutes. Therefore, the approach is suitable for the purpose of our research.

2. OBSERVATIONS AND MEASUREMENTS

In our previous studies, we evaluated the electric field of the reconnecting current sheet at the reconnection site, which reflects the reconnection rate per unit length along the current sheet with a two-dimensional assumption. In this study, we only evaluate the reconnection rate $\varphi_{\rm rec}$ and its time integration $\psi_{\rm rec} = \int \varphi_{\rm rec}(t)\, dt$, which does not require the two-dimensional assumption, thus avoiding large uncertainties in evaluating the ribbon expansion velocities. Figure 1 illustrates how the newly brightened pixels are counted from consecutive flare images and mapped to the co-registered longitudinal magnetogram obtained with the Michelson Doppler Imager (MDI). Uncertainties stemming from this method are evaluated by artificially misaligning the magnetogram and flare monograms by 1–2 pixels and by varying the cutoff value that outlines the edge of newly brightened patches. The former contributes to an error of no more than 10%, and the latter results in errors of 15%–20%. Altogether they give about 30% errors. Since flare observations are obtained at Hα and UV wavelengths reflecting emission from the chromosphere or transition region, we evaluate B_n by extrapolating the photospheric longitudinal magnetic fields to 2000 km above the photosphere using a potential field assumption. Most flares in this study occur on the disk with an orientation cosine factor of around 0.8. Systematic errors include calibration uncertainties and projection effects in MDI magnetograms, and the potential

[1] Big Bear Solar Observatory, New Jersey Institute of Technology, 40386 North Shore Lane, Big Bear City, CA 92314-9672.

[2] Division of Physics, Mathematics, and Astronomy, California Institute of Technology, 1200 East California Boulevard, Pasadena, CA 91125.

[3] Current address: Physics Department, Montana State University, Bozeman, MT 59717-3840; qiu@physics.montana.edu.

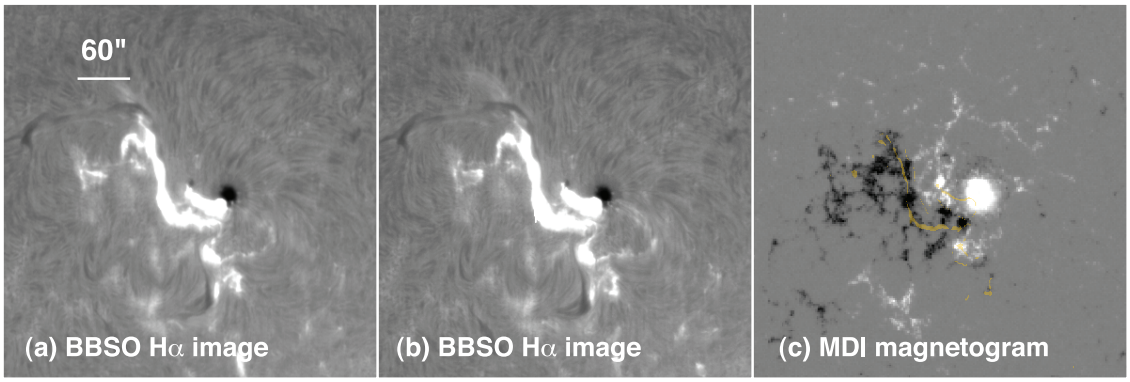

FIG. 1.—(*a*, *b*) Snapshots of a flare observed at Hα in consecutive time frames. (*c*) MDI longitudinal magnetogram (*gray scale*) with the newly brightened pixels (*gold symbols*) measured from (*a*) and (*b*) superposed.

field assumption in the extrapolation. These systematic uncertainties are more difficult to formulate and therefore not discussed in this Letter. However, we do not expect them to amount to altering the measurements by more than half an order of magnitude.

In this Letter, 13 events are analyzed. All of them consist of fast halo CMEs observed with LASCO C2 and C3 and C- to X-class flares observed in Hα and UV wavelengths with the Big Bear Solar Observatory and *Transition Region and Corona Explorer* (*TRACE*), respectively. Table 1 gives the information for the 13 events. Of these events, four were reported in earlier studies (Qiu et al. 2004; Jing et al. 2005 and references therein). Figure 2*a* gives the time profiles of the inferred reconnection rate derived in both the positive and negative magnetic fields for one event. In principle, the reconnection rates derived from the positive and negative magnetic fields, or φ^+ and φ^-, should be identical, as equal amounts of positive and negative magnetic flux participate in reconnection. But measurements do not always yield a good balance between the positive and negative fluxes (e.g., Fletcher & Hudson 2001). Figure 2*b* shows the ratio of total reconnection fluxes in opposite polarities, $R = \psi^+_{\rm rec}/\psi^-_{\rm rec}$, for all the 13 events. Given the uncertainties involved in the measurements, cases with $R \approx 0.5$–2 can be regarded as of good balance. Only two events in this study exhibit large imbalanced fluxes ($R > 2$ or $R < 0.5$). In this Letter, $\psi_{\rm rec}$ is given as the mean of $\psi^+_{\rm rec}$ and $\psi^-_{\rm rec}$.

The CME velocity $V_{\rm CME}$ is obtained from the LASCO online catalog.[4] It is computed from a linear fit to the height-time profile of the CME front measured with C2 and C3, i.e., with the assumption of constant CME speed. Errors in the CME velocity measurements are about 10% (S. Yashiro 2005, private communication). Note that these measurements give the CME velocities projected onto the plane of the sky.

We also distinguish these events by magnetic configurations of their source regions. Specifically, two events occur in quiescent regions with diffused weak magnetic fields that resemble the standard bipolar two-dimensional flare-CME picture, or CSHKP (Carmichael, Sturrock, Hirayama, Kopp, and Pneumann) model (Forbes & Acton 1996 and references therein), and the other events take place in active regions with complicated strong magnetic fields, typically at or around sunspots. Half of the events are accompanied by erupting filaments, while in the rest of the events, although filaments are present in source regions, they are not disrupted. We also note that in some events, postflare loops form above the undisrupted filaments (Fig. 3), which provides clear evidence that magnetic reconnection proceeds above the filament. These configurations are distinguished so as to provide observational tests of existing CME models, for example, the catastrophe flux cancellation model (e.g., Forbes & Priest 1995) versus the breakout model (e.g., Antiochos et al. 1999).

[4] See http://cdaw.gsfc.nasa.gov/CME_list for more details.

TABLE 1
FLARE AND CME INFORMATION

Date	Source Region[a]	Flare Magnitude[b]	Erupting Filament	Reconnection Flux[c] (10^{21} Mx)	CME Velocity[d] (km s^{-1})
1998 Nov 5	AR	M8.3	Yes	3.3 ± 0.5	1118
2000 Sep 12	QS	M1.0	Yes	3.7 ± 0.6	1550
2000 Nov 24	AR	X1.0	Yes	1.5 ± 0.3	1000
2001 Oct 19	AR	X1.6	Yes	2.6 ± 0.5	970
2002 Nov 24	QS	C6.4	Yes	1.8 ± 0.8	1077
2003 Oct 28	AR	X17.0	Yes	17.3 ± 2.1	2459
1998 Apr 29	AR	M6.8	No	3.7 ± 0.4	1374
2001 Sep 28	AR	M3.3	No	3.9 ± 0.4	846
2002 Mar 20	AR	C4.0	No	1.4 ± 0.3	603
2002 Jul 26	AR	M8.7	No	2.5 ± 0.8	818
2003 Oct 29	AR	X10.0	No	10.2 ± 1.0	2029
2004 Nov 7	AR	X2.0	No	5.4 ± 0.7	1759
2005 May 13	AR	M8.0	No	6.2 ± 0.4	1689

[a] AR = active region; QS = quiet Sun.
[b] According to *GOES* categorization of flares.
[c] Magnetic fields measured from MDI are multiplied by a scaling factor of 1.56 (Berger & Lites 2003).
[d] Obtained from http://cdaw.gsfc.nasa.gov/CME_list.

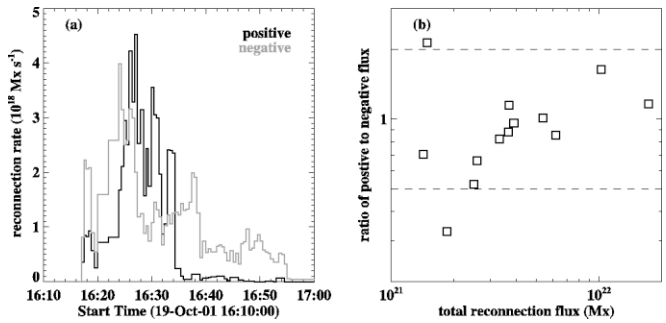

FIG. 2.—(*a*) Magnetic reconnection rate derived in positive and negative magnetic fields for one flare event. (*b*) Ratio (R) of total reconnection flux derived in positive magnetic fields to that in negative magnetic fields for 13 events. Dashed lines indicate $R = 0.5$ and 2.

3. RESULTS

Figure 4 shows the scatter plot of $V_{\rm CME}$ versus $\psi_{\rm rec}$ for the 13 events analyzed. A proportionality between $V_{\rm CME}$ and $\psi_{\rm rec}$ is evident in the figure. The linear cross-correlation is computed to be 89% for the 13 pairs of data, yielding a confidence level of greater than 99.5%. Considering the imbalance between positive and negative reconnection fluxes from the measurements, we can also compare the larger, rather than the mean, of $\psi^{+}_{\rm rec}$ and $\psi^{-}_{\rm rec}$ with $V_{\rm CME}$. This slightly deduces the degree of correlation by 1%. That is to say, a greater amount of reconnection flux is related to larger CME velocities out of the fast acceleration stage.

Note that events with a greater amount of reconnection flux as well as larger CME velocities do not necessarily originate from complicated active regions with strong magnetic fields. For example, for the events on 2000 September 12 and 2002 November 24, the source regions are dominated by very simple bipolar fields, the maximum magnetic field strength being no more than 400 G. The magnitudes of the reconnection rate and acceleration are not very large. But the durations of reconnection and acceleration are very long, giving rise to rather large mean CME velocities at ~1000–1500 km s^{-1}. In comparison, some events occur in much stronger magnetic fields with a maximum field strength over 1000 G, but the durations of acceleration and reconnection are short, leading to mean CME velocities around 1000 km s^{-1}, comparable to the events in simple and weak-field regions. The couple of events with relatively slow CMEs ($V_{\rm CME} < 1000$ km s^{-1}) in this study originate from active regions. That both the magnitude and duration of CME acceleration are important properties is also suggested by a recent independent study (Zhang 2005) investigating the kinematic behavior of several tens of CMEs observed from LASCO C1 to C3.

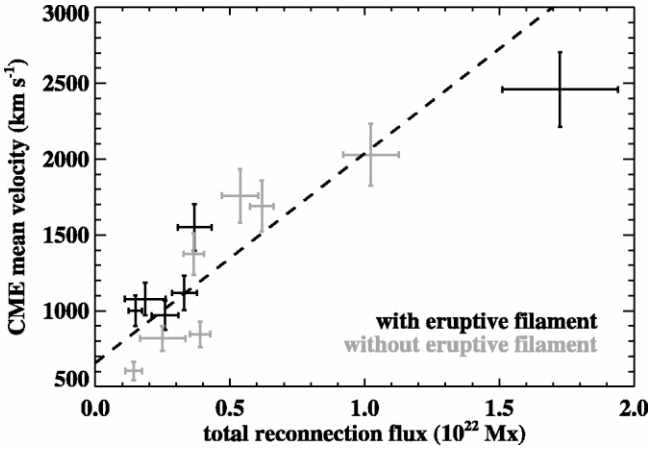

FIG. 4.—Scatter plot of CME velocities vs. total reconnection flux for 13 events. Dark and gray colors indicate events associated with erupting and nonerupting filaments, respectively. The dashed guideline shows the least-squares linear fit to the data points.

Furthermore, events associated with and without erupting filaments are distinguished by dark and gray symbols in Figure 4. However, they do not appear to be two populations in the scatter plot. Therefore, at least at this level, the specific magnetic configuration does not play a significant role. These results substantiate the suggestion by Qiu et al. (2004) and Qiu (2005) that CME velocities, and consequently the kinematic energy of CMEs, might not depend on particular magnetic configurations in source regions.

The measured $\psi_{\rm rec}$ amounts to 10^{21}–10^{22} Mx. These values should be regarded as the lower limits of the total amount of magnetic flux participating in magnetic reconnection, as the numerical method takes into account relatively strong brightenings in flare core regions. However, reconnection flux involved in other than core regions is negligible, as remote brightenings usually occur in weak magnetic fields and are transient in comparison with flares in core regions.

4. CONCLUSION

We find a scaling relationship between velocities of CMEs, observed by LASCO C2 and C3, and total reconnection flux, amounting to 10^{21}–10^{22} Mx, evaluated from flare observations for 13 events analyzed in this Letter. The result confirms the importance of magnetic reconnection in the early stage of CMEs. The events in our analysis occur in source regions with

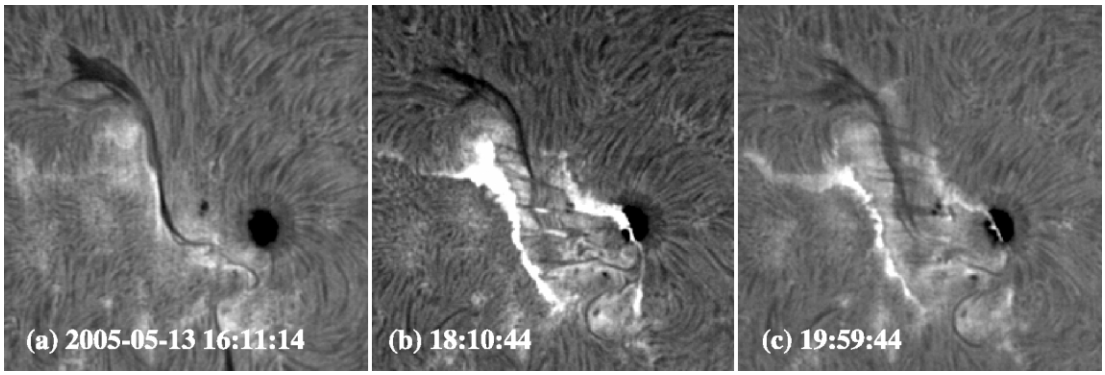

FIG. 3.—Snapshots of (*a*) preflare and (*b*, *c*) postflare images taken at Hα showing the undisrupted filament between flare ribbons and postflare loops formed above the filament.

different magnetic configurations; however, this cannot be distinguished in the velocity-flux plot. This result indicates that the specific magnetic configuration might not be important in generating CMEs with certain speeds, and that CME kinematic energies are likely independent of magnetic configurations in the low corona.

In general, dynamics of solar ejecta are believed to be determined by the Lorentz and pressure forces (Vršnak 1990; Chen 1996), the former being related to the amount of magnetic flux confined in the erupted field. Research thus far has been conducted to explore the relationship between magnetic flux measured in situ in magnetic clouds and the dynamics of solar ejecta. Dal Lago et al. (2001) and Owens & Cargill (2002) reported that the intensity of the magnetic fields in magnetic clouds is related to the turbulence velocity of the solar wind. Earlier, Lindsay et al. (1999) concluded that interplanetary magnetic fields (IMFs) with larger maximum magnitudes are associated with high-speed CMEs. Very recently, Yurchyshyn et al. (2004, 2005) found that the magnitudes of the hourly averaged B_z component and the total IMF B_{tot} are both scaled with the speed of CMEs launched around the solar disk center. Our study, for the first time, illustrates the relationship between the CME velocity and magnetic flux transferred between the flux rope and its ambient fields on the Sun's surface by means of magnetic reconnection. A significant amount of the reconnection flux is expected to become part of the expanding flux rope, which travels into interplanetary space.

The CME catalog is generated and maintained by the Center for Solar Physics and Space Weather, the Catholic University of America in cooperation with the Naval Research Laboratory, and NASA. The *Solar and Heliospheric Observatory* (*SOHO*) is a project of international cooperation between ESA and NASA. *TRACE* is a NASA Small Explorer (SMEX) mission. We acknowledge using data from the Global High-Resolution Hα Network, operated by Big Bear Solar Observatory, New Jersey Institute of Technology. J. Q. is supported by NASA grant NNG04GF07G and NSF grant ATM 04-54606. V. B. Y. is supported by NSF grants ATM 99-03515 and ATM 02-05157, and NASA grant NAG5-9682.

REFERENCES

Antiochos, S. K., DeVore, C. R., & Klimchuk, J. A. 1999, ApJ, 510, 485
Berger, T. E., & Lites, B. W. 2003, Sol. Phys., 213, 213
Chen, J. 1996, J. Geophys. Res., 101, 27499
Dal Lago, A., Gonzalez, W. D., de Gonzalez, A. L. C., & Vieira, L. E. A. 2001, J. Atmos. Sol.-Terr. Phys., 63, 451
Fletcher, L., & Hudson, H. 2001, Sol. Phys., 204, 69
Forbes, T. G., & Acton, L. W. 1996, ApJ, 459, 330
Forbes, T. G., & Lin, J. 2000, J. Atmos. Sol.-Terr. Phys., 62, 1499
Forbes, T. G., & Priest, E. R. 1995, ApJ, 446, 377
Jing, J., Qiu, J., Lin, J., Qu, M., Xu, Y., & Wang, H. 2005, ApJ, 620, 1085
Lindsay, G. M., Luhmann, J. G., Russell, C. T., & Gosling, J. T. 1999, J. Geophys. Res., 104, 12515
Owens, M. J., & Cargill, P. J. 2002, J. Geophys. Res., 107, 1050
Qiu, J. 2005, J. Atmos. Sol.-Terr. Phys., submitted
Qiu, J., Wang, H., Cheng, C. Z., & Gary, D. E. 2004, ApJ, 604, 900
Vršnak, B. 1990, Sol. Phys., 129, 295
Yurchyshyn, V., Hu, Q., & Abramenko, V. 2005, Space Weather, 3, S08C02, doi: 10.1029/2004SW000124
Yurchyshyn, V., Wang, H., & Abramenko, V. 2004, Space Weather, 2, S02001, doi: 10.1029/2003SW000020
Zhang, J. 2005, in IAU Symp. 226, Coronal and Steller Mass Ejections, ed. K. Dere, J. Wang, & Y. Yan (Cambridge: Cambridge Univ. Press), 65
Zhang, J., Dere, K. P., Howard, R. A., Kundu, M. R., & White, S. M. 2001, ApJ, 559, 452